H. Shangguan, L. W. Casperson, A. Shearin, D. L. Paisley and S. A. Prahl, "Effects of Material Properties on Laser-induced Bubble Formation in Absorbing Liquids and On Submerged Targets," *Diagnostic and Therapeutic Cardiovascular Interventions VII*, D. L. Paisley and A. M Frank Eds., Proc. SPIE 2869, 783–791, (1997).

Effects of Material Properties on Laser-induced Bubble Formation in Absorbing Liquids and On Submerged Targets

HanQun Shangguan,[1,2] Lee W. Casperson,[1] Alan Shearin,[2]

Dennis Paisley,[4] and Scott A. Prahl[2,3]

[1]Portland State University, Department of Electrical Engineering, Portland, OR 97207
[2]Oregon Medical Laser Center, Portland, OR 97225
[3]Oregon Health Sciences University, Portland, OR 97201
[4]Los Alamos National Laboratory, Los Alamos, NM 87545

Abstract

Pulsed laser ablation of blood clots in a fluid-filled blood vessel is accompanied by an explosive evaporation process. The resulting vapor bubble rapidly expands and collapses to disrupt the thrombus (blood clot). The hydrodynamic pressures following the bubble expansion and collapse can also be used as a driving force to deliver clot-dissolving agents into thrombus for enhancement of laser thrombolysis. Thus, the laser-induced bubble formation plays an important role in the thrombus removal process. In this study the effects of material properties on laser-induced cavitation bubbles formed in liquids and on submerged targets have been visualized with a microsecond strobe or high speed framing camera.

Keywords: laser-induced vapor bubble, localized drug delivery, high speed photography, hydrodynamic pressure

1 Introduction

Interest in cavitation bubbles in liquids initially arose from their destructive action on ship propellers and in hydraulic machinery. Cavitation erosion is attributed to the action of acoustic transients emitted during bubble collapse and to the impingement of the high-speed liquid jet that develops when a bubble collapses in the vicinity of a solid boundary.[1] It was shown soon after the invention of laser that cavitation occurs in a liquid when irradiated with laser light.[2] This form of cavitation is called optical cavitation.

Laser-induced cavitation bubbles have been used in ophthalmology, cardiology, and urology. For example, laser pulses produce a plasma with subsequent bubble formation for ocular surgery by photodisruption.[3] Laser-induced lithotripsy fragments kidney stones through cavitation erosion.[4] Laser pulses have been used to remove thrombus in obstructed arteries.[5] In a previous study, we demonstrated that the laser-induced hydrodynamic pressures arising from the cavitation bubble expansion and collapse could also drive drug into thrombus.[6]

It has been established that a cavitation bubble can be generated at a fiber tip or on an ablation target

depending on where the laser energy is absorbed. A cavitation bubble is formed at the fiber tip if a laser pulse is delivered into an absorbing liquid (e.g., blood or saline). The bubble is formed on thrombus if a fluid-core catheter is used to wash away ambient blood, so that a 480 nm or 577 nm laser pulse can be absorbed by thrombus.[7,8]

Photomechanical drug delivery uses a laser pulse to generate a cavitation bubble in a blood vessel due to the absorption of laser energy by surrounding liquids or targets. The cavitation bubble expands and collapses within a millisecond of the delivery of the laser pulse. The hydrodynamic pressure following the bubble formation can drive drugs into thrombus. One can perform photomechanical drug delivery by timing the laser pulse to be coincident with an injected bolus of drug. A concern for photomechanical drug delivery is whether bubble dynamic behavior changes when the bubbles form in absorbing liquids with different physical properties or on ablation targets with different mechanical strengths.

Although several studies have focused on the laser-induced cavitation bubble dynamics,[9–11] no detailed study has been done on the dynamic behavior of laser-induced cavitation bubbles formed in absorbing liquids with different physical properties or on ablation targets with different mechanical strengths with the pulsed dye laser. The aim of this study was to investigate the effects of materials on the bubble formation in absorbing liquids or on soft targets with time-resolved flash photography and high-speed photography.

2 Materials and Methods

2.1 Sample Preparations

2.1.1 Absorbing Soft Targets

Thrombus was simulated using 3.5–5% gelatin (60–300 bloom, Sigma Chemicals). The percentage was determined by the weight ratio of gelatin to water. The bloom number is the standard method for indicating the toughness of gelatins and is a measure of surface tension. Higher bloom numbers indicate stronger gelatins. No attempt was made to correlate the bloom number with the strength of any specific clots in this study, although the range studied was similar to that of typical clot toughness. The gelatin-water mixture was heated to 60°C with stirring until it became clear. Liquid gelatin samples were poured into 1 cm cuvettes and molded to form 2–3 cm thick thrombus models with flat surfaces. Dye solution (0.07 g of Blue 15 from Sigma in 40 ml water) was placed on the gelatin surface for 5 minutes and a blue layer ($\sim$300 μm thick with a $\sim$100 cm^{-1} absorption coefficient at 577 nm) was formed. At 504 nm, 300 cm^{-1} gelatin samples were made by adding 0.3 g of Direct Red 81 from Sigma in 100 ml of liquid gelatin (3.5% 175 bloom).

2.1.2 Absorbing Liquids

Two liquids (water and mineral oil) were used in this study. Dyes (Direct Red 81 from Sigma and D&C Red #17 from Warner-Jenkinson) were added to water and oil respectively to achieve desired absorption. Both of the dyes were photostable and had a peak absorption around 504 nm. The absorption coefficients of the solutions had a nearly linear relationship with the concentration of dye in the solutions: 0.0837 g of Direct Red 81 in 30 ml water gave an absorption coefficient of 300 cm^{-1}, while 0.0367 g of D&C Red #17 was added into 30 ml oil to obtain the same absorption. Direct Red 81 dye was easily dissolved in water after stirring several minutes at room temperature ($\sim$25°C). Heating was needed to make the oil solutions. The dye-oil mixture was heated to 100°C with stirring until the appearance became uniform, and then cooled down to room temperature before the experiments.

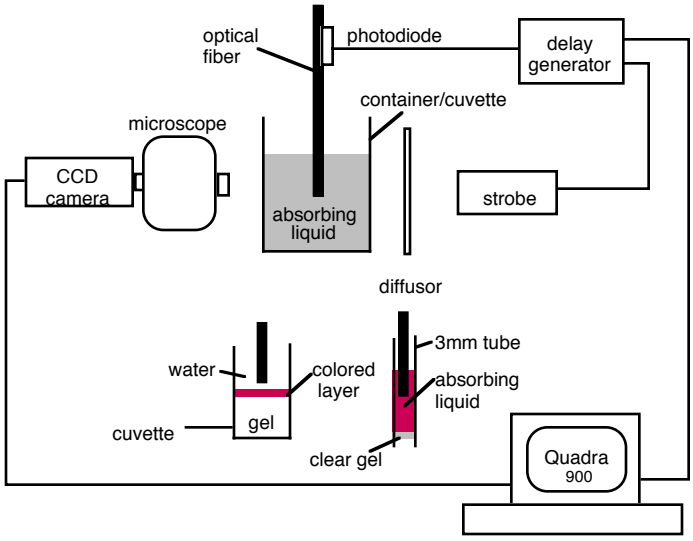

Figure 1: Schematic of experimental setup for flash photography

2.2 Laser Irradiation

Laser irradiation at 504 or 577 nm was provided by flashlamp excited dye lasers (Palomar Medical Technologies). The pulse duration was $\sim$1.3 μs (full width at half maximum). The laser pulses were delivered into absorbing liquids or through clear liquids onto thrombus phantoms via a fused-silica fiber with diameters 300 and 1000 μm. The energy per pulse was measured with an joulemeter (Molectron). Pulse-to-pulse energy variation was less than 5%.

2.3 Photographic Systems

Two photographic systems were used to visualize the bubble formation. A time-resolved flash photographic setup provided a series of single stroboscopic pictures, while a high-speed framing camera captured 12 images for one single event. The bubble sizes were measured directly from the images by using the optical fiber in each image as a scale factor. The images were analyzed using NIH Image or IP Lab software.

2.3.1 Flash Photography

The microsecond time-resolved flash photography setup is shown in Figure 1. The processes taking place at the fiber end or on the gelatin surface were photographed using a triggerable CCD camera (CV-251, Protec). A stereomicroscope (SZ60, Olympus) was used for magnification. Each picture was a single event and was repeated three times for each parameter set. The bubble size was reproducible to 5% before the bubble collapse. The appearance of cavitation bubbles varied widely after the bubble collapse. A strobe (MVS–2601, EG&G) with a 5 μs pulse duration (full width at half-maximum) was used for illumination. The delay times were controlled by a digital delay generator (DG535, Stanford Research Systems). The generator was triggered by the laser pulse by using a photodiode (UDT Instruments) that was attached to the laser delivery fiber, so flash photographs were taken at variable delay times of 5–500 μs after the laser pulse. A laser filter was positioned in front of the microscope to avoid blinding the CCD camera.

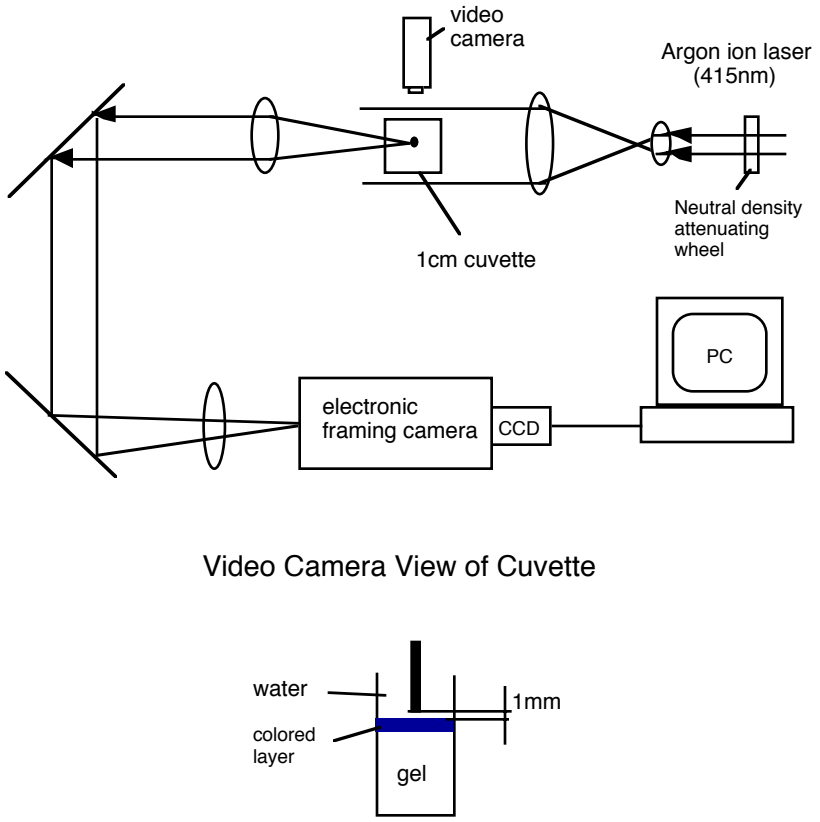

Figure 2: Schematic of high-speed shadowgraph system.

2.3.2 High-speed Shadowgraph

Figure 2 shows a schematic of the high-speed photographic system. A continuous-wave argon ion laser at 514 nm was used for illumination. The laser beam was expanded to 10 mm diameter using a 3× beam expanding telescope for illuminating the sample area. A shadowgraph of the sample surface and optical fiber was imaged on the input of an electronic framing camera (FS501, Ultranac). By properly timing the pulsed-dye laser and argon ion laser with the triggering of the electronic framing camera, multiple exposures of the interaction of the laser pulse with the thrombus could be realized. The ablation process could be examined from start as early as several hundred nanoseconds to several hundred microseconds after the laser pulse. The electronic framing camera captured 12 pictures with an adjustable interframe time. The photographs were taken with one microsecond exposure time and 25 microsecond interframe time. The 12 frames were captured on a 1152×770 pixel CCD chip with the image read directly into a PC for data analysis. The illumination light was adjusted using a neutral density wheel (50G00AV.2, Newport).

2.4 Experiments

Three experiments were performed to investigate the effects of materials:

1. Does viscosity and density of absorbing liquids affect the bubble size formed in absorbing liquids?

Liquid	Density mg/mm^3	Viscosity cP	Bubble Width in Liquid mm	Bubble Width on Gelatin mm
Water	0.992	0.653	3.9	5.5±0.2
Mineral oil	0.86	29.67	2.2	5.4±0.2
Contrast Medium	1.411	13.34	—	5.2±0.3

Table 1: Variation in maximum bubble size when formed *in* 300 cm^{-1} liquids or under clear liquids *on* 300 cm^{-1} gelatin. The bubbles formed in liquids were confined by a 3 mm tube, and consequently are smaller than bubbles formed in 1 cm cuvettes because of the presence of tube boundaries. The errors are the standard deviation of three measurements.

2. What are the differences when the bubble forms on a soft target covered with the liquids?

3. Does the mechanical strength of the ablation targets affect the bubble dynamics?

In the first experiment, single pulses of 100 mJ were delivered into an oil solution or water solution through a 1000 μm fiber. The absorption coefficient for both solutions was 300 cm^{-1}. The solutions filled a 3 mm diameter silicone tube and the fiber was centered inside the tube. The laser emitted light with a wavelength 504 nm.

In the second experiment, two sets of experiments were performed. The first set used single pulses of 50 mJ were delivered onto 100 cm^{-1} gelatin through clear water or clear oil via a 300 μm fiber placed 1 mm above the gelatin surface. The bubble formation was visualized using high-speed shadowgraphy. The laser emitted 577 nm light. The second set used 100 mJ laser pulses to irradiate the gelatin sample (300 cm^{-1}) through clear water, clear mineral oil (Paddock Lab), and clear contrast medium (MD-76, Mallinckrod Medical, Inc.) using a 1000 μm fiber that was 1 mm away from the gelatin surface. The bubble width was measured 300 μs after the laser pulse with flash photography. The laser operated at 504 nm. The density and viscosity for water, mineral oil, and contrast medium are summarized in Table 1.

The third experiment visualized the bubble formation on 100 cm^{-1} gelatin with different mechanical strengths. Single pulses of 50 mJ pulse were delivered via a 300 μm fiber onto a gelatin sample (100 cm^{-1}) with varied hardness (3.5% 60 bloom and 5% 300 bloom) under water. The fiber tip was 1 mm above the gelatin surface and centered inside 1 cm cuvette. The laser operated at 577 nm.

3 Results

The cavitation bubble dimensions were significantly different when the bubble was formed in the 300 cm^{-1} oil solution (Figure 3a) compared with those formed in the 300 cm^{-1} water solution (Figure 3b). The maximum bubble width formed in the water solution was larger than that formed in the oil solution by a factor of 1.8 (i.e., 3.9 mm in water and 2.2 mm in oil). The bubble formed in 300 cm^{-1} oil reached its maximum size 50 μs after the laser pulse and dilated the tube wall by 10%. The subsequent bubble collapse caused a 4% invagination of the tube wall. In 300 cm^{-1} water, the maximal dilation of 29% was 60 μs and the tube diameter was reduced by 13% at 900 μs due to the collapse.

Figure 4 shows the bubble width generated on the absorbing gelatin surface under clear water and oil. There were no significant differences in bubble sizes formed on the gelatin under water or oil. The bubble heights did not differ significantly from the widths. Note that the bubble in water grew faster initially (~25 μs) and at 50 μs they

matched. Flash photographs revealed that the bubble dimensions formed under water, oil, and contrast medium were quite similar each other. The measurements are summarized in Table 1. We observed that a stream of color released from the absorbing gelatin surface when the contrast medium interacted with the gelatin samples. This was not observed for water and oil.

Two sets of high-speed shadowgraphs are shown in Figure 5. The bubble widths from Figure 5 are plotted as a function of delay time in Figure 6. In the case of soft 3.5% 60 bloom gelatin, the bubble shape was spherical during expansion and contraction (Figure 5a). The bubble shape became elliptical after 175 μs of the delivery of the laser pulse when the harder 5% 300 bloom gelatin was used (Figure 5b).

4 Discussion

This study investigated the effects of density, viscosity, and mechanical strength on laser-induced cavitation bubbles formed in absorbing liquids or on absorbing gelatin submerged in clear liquids. This study demonstrated that the effects of density and viscosity of the liquids above the target on the bubble formation are negligible when the bubble formed on an ablation target (Figure 4 and Table 1). The mechanical strength of the target material does affect the bubble dynamics (Figure 6). The bubble dynamics strongly depended on the physical properties of the absorbing liquid when the bubble formed in an absorbing liquid (Table 1).

The flash photographs revealed that the larger bubble formed in water could cause greater dilation of the tube wall (Figure 3). A study by de la Torre and Gregory suggested that laser-induced cavitation bubble could cause dissections in vascular tissue during pulsed-dye laser angioplasty.[12] Reducing bubble dimensions has been proposed to minimize the photomechanical effect.[10,11,13] This study suggests that the bubble size may be reduced by using a liquid in which small bubbles are formed like oil rather than water.

The density and viscosity of clear liquids do not affect bubble dynamics significantly when the bubble is formed on gelatin. This implies that the bubble formation depends on the material properties of the ablation target. This finding suggests that photomechanical drug delivery may be achieved by using any drugs that are suitable to dissolve the thrombus during laser thrombolysis regardless of the density and viscosity of the drug.

Previous studies have demonstrated that the mechanical properties of tissue significantly affect the ablation rate and the bubble formation.[11,14] However, there is no evidence available to show that the mechanical strength of the thrombus affects the bubble dynamics. This study provided evidence that the mechanical strength of the ablation targets affects the bubble dynamics and suggests that the mechanical strength of the thrombus should be considered when modelling the bubble dynamics during laser thrombolysis and photomechanical drug delivery.

In conclusion, the bubble formation was relatively independent of the liquid properties when the bubbles were formed on the ablation targets under clear liquids. The bubble formation in absorbing liquids strongly depended on the material properties. The mechanical strength of the ablation targets affected the bubble geometry, and the bubble became more elliptical after it reached its maximal dimension for the harder targets.

5 Acknowledgements

H. Shangguan thanks the organizing committee of the 22nd International Congress on High-Speed Photography and Photonics, SPIE, and the National Science Foundation for a Student Travel Award. The authors wish to thank Dr. R. E. Hermes of the Los Alamos National Laboratory for his valuable discussion and D. B. Stahl at the Los Alamos National Laboratory for assistance with high-speed shadowgraphy. This work was supported in part by the Murdock Foundation, Portland, Oregon, and the Whitaker Foundation, Washington, DC.

6 REFERENCES

[1] Y. Tomita and A. Shima, "Mechanisms of impulsive pressure generation and damge pit formation by bubble collapse," *J. Fluid Mech.*, vol. 169, pp. 535–564, 1986.

[2] R. G. Brewer and K. E. Rieckhoff, "Stimulated Brillouin scattering in liquids," *Phys. Rev. Lett.*, vol. 13, pp. 334–336, 1964.

[3] A. Vogel, S. Busch, K. Jungnickel, and R. Birngruber, "Mechanisms of intraocular photodisruption with picosecond and nanosecond laser pulses," *Lasers Surg. Med.*, vol. 15, pp. 32–43, 1994.

[4] K. Rink, G. Delacrétaz, and R. P. Salathé, "Fragmentation process of current laser lithotriptors," *Lasers Surg. Med.*, vol. 16, pp. 134–146, 1995.

[5] K. Gregory, "Laser thrombolysis," in *Interventional Cardiology* (E. J. Topol, ed.), vol. 2, ch. 5, pp. 892–902, W. B. Saunders Company, 1994.

[6] H. Shangguan, L. W. Casperson, A. Shearin, K. W. Gregory, and S. A. Prahl, "Drug delivery with microsecond laser pulses into gelatin," *Appl. Opt.*, vol. 35, pp. 3347–3357, 1996.

[7] K. W. Gregory and R. R. Anderson, "Liquid core light guide for laser angioplasty," *IEEE J. Quantum Electron.*, vol. 26, pp. 2289–2296, 1990.

[8] U. S. Sathyam, A. Shearin, E. A. Chasteney, and S. A. Prahl, "Threshold and ablation efficiency studies of microsecond ablation of gelatin under water," *Lasers Surg. Med.*, vol. 19, 1996 (in press).

[9] A. Vogel, W. Lauterborn, and R. Timm, "Optical and acoustic investigations of the dynamics of laser-produced cavitation bubbles near a solid boundary," *J. Fluid Mech.*, vol. 206, pp. 299–238, 1989.

[10] T. G. van Leeuwen, E. D. Jansen, A. J. Welch, and C. Borst, "Excimer laser induced bubble: Dimensions, theory, and implications for laser angioplasty," *Lasers Surg. Med.*, vol. 18, pp. 381–390, 1996.

[11] E. D. Jansen, T. Asshauer, M. Frenze, M. Motamedi, G. Delacretaz, and A. J. Welch, "Effect of pulse duration on bubble formation and laser-induced pressure waves during holmium laser ablation," *Lasers Surg. Med.*, vol. 18, pp. 278–293, 1996.

[12] R. de la Torre and K. W. Gregory, "Cavitation bubbles and acoustic transients may produce dissections during laser angioplasty," *J. Am. Coll. Cardiol.*, vol. 19A, p. 48, 1992.

[13] A. Vogel, R. Engelhardt, U. Behnle, and U. Parlitz, "Minimization of cavitation effects in pulsed laser ablation - illustrated on laser angioplasty," *Appl. Phys. B*, vol. 62, pp. 173–182, 1996.

[14] J. T. Walsh Jr. and T. F. Deutsch, "Pulsed CO_2 laser ablation of tissue: Effect of mechanical properties," *IEEE Trans. Biomed. Eng.*, vol. 36, pp. 1195–1201, 1989.

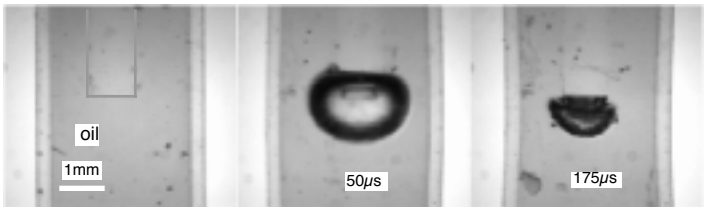

(a)

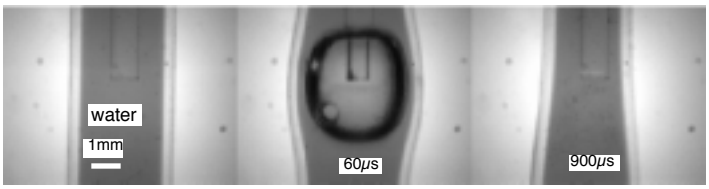

(b)

Figure 3: Side view of bubble formation in a 3 mm silicone filled with (a) the 300 cm^{-1} oil solution and (b) the 300 cm^{-1} water solution. Single pulses of 100 mJ were delivered via a 1000 μm fiber.

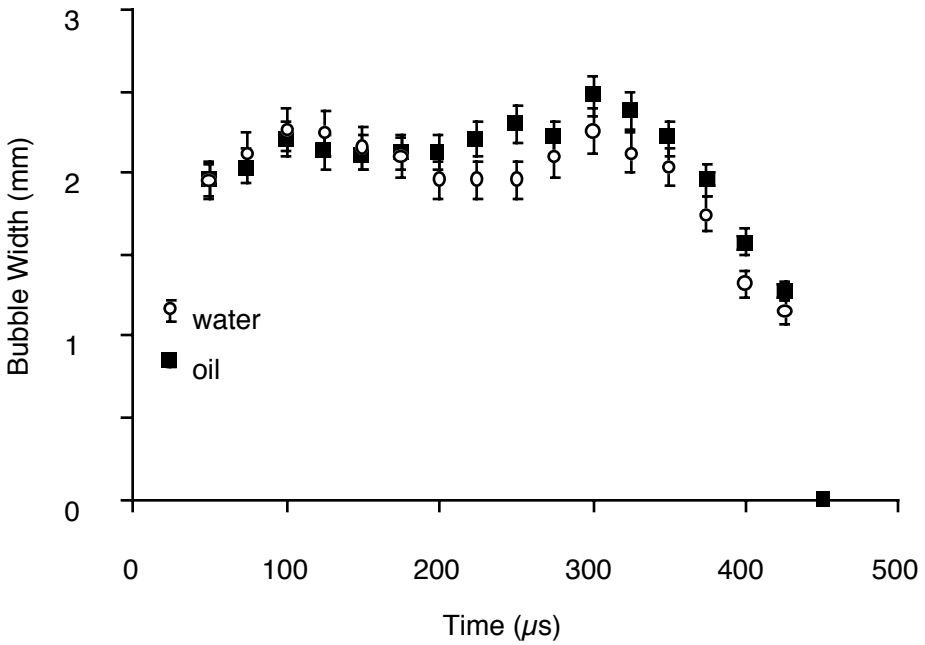

Figure 4: Measured bubble diameter as function of time. Single pulses of 50 mJ were delivered onto the absorbing gelatin surface (100 cm^{-1}) through clear water and oil via a 300 μm fiber. The fiber tip was 1 mm above the gelatin surface. Error bars represent the standard deviation of three measurements.

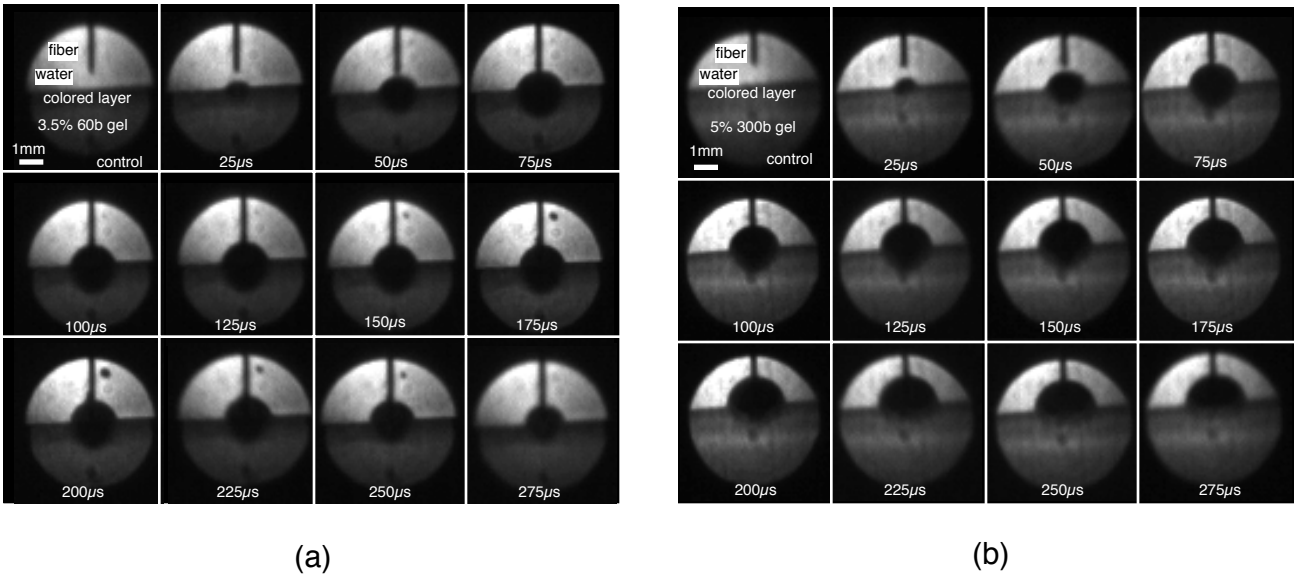

Figure 5: Shadowgraphs of bubble formation on the $100\,\mathrm{cm}^{-1}$ gelatin samples with different mechanical strengths: (a) 3.5% 60 bloom and (b) 5% 300 bloom. Single pulses of 50 mJ were delivered onto the gelatin surface through clear water via a $300\,\mu$m fiber. The fiber tip was 1 mm above the surface.

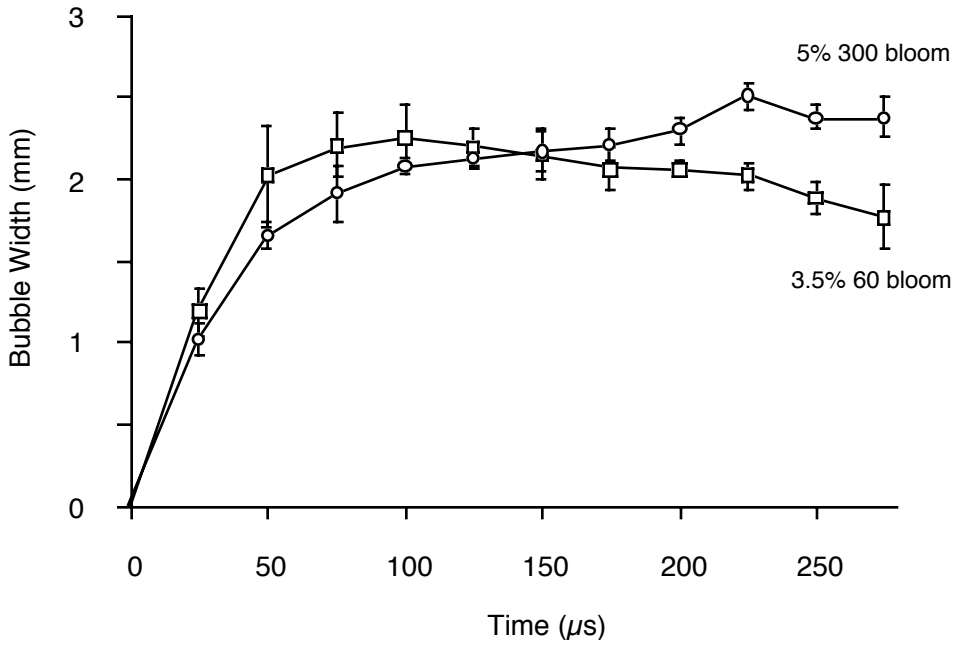

Figure 6: The bubble width as function of time after the laser pulse for 3.5% 60 bloom gelatin and 5% 300 bloom gelatin. Error bars represent the standard deviation of three measurements.